

Original Article

Continuous exposure to α -glycosyl isoquercitrin from developmental stages to adulthood is necessary for facilitating fear extinction learning in rats

Yasunori Masubuchi^{1,2}, Junta Nakahara¹, Satomi Kikuchi^{1,3}, Hiromu Okano^{1,3}, Yasunori Takahashi^{1,3}, Kazumi Takashima^{1,3}, Mihoko Koyanagi⁴, Robert R. Maronpot⁵, Toshinori Yoshida^{1,3}, Shim-mo Hayashi⁴, and Makoto Shibutani^{1,3,6,*}

¹ Laboratory of Veterinary Pathology, Tokyo University of Agriculture and Technology, 3-5-8 Saiwai-cho, Fuchu-shi, Tokyo 183-8509, Japan

² Pathogenetic Veterinary Science, United Graduate School of Veterinary Sciences, Gifu University, 1-1 Yanagido, Gifu-shi, Gifu 501-1193, Japan

³ Cooperative Division of Veterinary Sciences, Graduate School of Agriculture, Tokyo University of Agriculture and Technology, 3-5-8 Saiwai-cho, Fuchu-shi, Tokyo 183-8509, Japan

⁴ Global Scientific and Regulatory Affairs, San-Ei Gen F.F.I., Inc., 1-1-11 Sanwa-cho, Toyonaka-shi, Osaka 561-8588, Japan

⁵ Maronpot Consulting, LLC, 1612 Medfield Road, Raleigh, North Carolina 27607, USA

⁶ Institute of Global Innovation Research, Tokyo University of Agriculture and Technology, 3-5-8 Saiwai-cho, Fuchu-shi, Tokyo 183-8509, Japan

Abstract: We previously reported that exposure to α -glycosyl isoquercitrin (AGIQ) from the fetal stage to adulthood facilitated fear extinction learning in rats. The present study investigated the specific AGIQ exposure period sufficient for inducing this behavioral effect. Rats were dietarily exposed to 0.5% AGIQ from the postweaning stage to adulthood (PW-AGIQ), the fetal stage to postweaning stage (DEV-AGIQ), or the fetal stage to adulthood (WP-AGIQ). Fear memory, anxiety-like behavior, and object recognition memory were assessed during adulthood. Fear extinction learning was exclusively facilitated in the WP-AGIQ rats. Synaptic plasticity-related genes showed a similar pattern of constitutive expression changes in the hippocampal dentate gyrus and prelimbic medial prefrontal cortex (mPFC) between the DEV-AGIQ and WP-AGIQ rats. However, WP-AGIQ rats revealed more genes constitutively upregulated in the infralimbic mPFC and amygdala than DEV-AGIQ rats, as well as FOS-immunoreactive(+) neurons constitutively increased in the infralimbic cortex. Ninety minutes after the last fear extinction trial, many synaptic plasticity-related genes (encoding Ephs/Ephrins, glutamate receptors/transporters, and immediate-early gene proteins and their regulator, extracellular signal-regulated kinase 2 [ERK2]) were upregulated in the dentate gyrus and amygdala in WP-AGIQ rats. Additionally, WP-AGIQ rats exhibited increased phosphorylated ERK1/2⁺ neurons in both the prelimbic and infralimbic cortices. These results suggest that AGIQ exposure from the fetal stage to adulthood is necessary for facilitating fear extinction learning. Furthermore, constitutive and learning-dependent upregulation of synaptic plasticity-related genes/molecules may be differentially involved in brain regions that regulate fear memory. Thus, new learning-related neural circuits for facilitating fear extinction can be established in the mPFC. (DOI: 10.1293/tox.2020-0025; J Toxicol Pathol 2020; 33: 247–263)

Key words: α -glycosyl isoquercitrin (AGIQ), fear extinction learning, synaptic plasticity, phosphorylated ERK1/2, rat

Introduction

Alpha-glycosyl isoquercitrin (AGIQ), also known as enzymatically modified isoquercitrin, is a polyphenolic flavonol glycoside derived by the enzymatic glycosylation of rutin, which is found in several plant species such as buckwheat (*Fagopyrum esculentum* Moench), rue (*Ruta graveolens* L.), and Japanese pagoda tree (*Sophora japonica* L.)¹. AGIQ is a mixture of quercetin glycoside, consisting of isoquercitrin and its α -glucosylated derivatives, with 1–10 or more additional linear glucose moieties¹. AGIQ is highly water soluble and has antioxidant potential^{1, 2}. AGIQ has been reported to exert antioxidant effects³ and to have anti-

Received: 22 April 2020, Accepted: 20 July 2020

Published online in J-STAGE: 13 August 2020

*Corresponding author: M Shibutani

(e-mail: mshibuta@cc.tuat.ac.jp)

©2020 The Japanese Society of Toxicologic Pathology

This is an open-access article distributed under the terms of the Creative Commons Attribution Non-Commercial No Derivatives

(by-nc-nd) License. (CC-BY-NC-ND 4.0: <https://creativecommons.org/licenses/by-nc-nd/4.0/>).



inflammatory³, anti-hypertensive⁴, anti-allergic⁵, and tumor suppressive⁶ properties. It has been found to be safe in a 90-day toxicity study⁷ and in genotoxicity assays⁸.

Recently, we reported that continuous exposure to 0.5% AGIQ in the diet from the fetal period through adulthood in rats facilitated fear extinction learning on the contextual fear conditioning test. Additionally, it facilitated the adult transcript upregulation of *Fos*, which encodes Fos proto-oncogene, AP-1 transcription factor subunit (FOS); *Kif21b*, which encodes kinesin family member 21B (KIF21B) in the hippocampal dentate gyrus; and *Grin2d*, which encodes glutamate ionotropic receptor *N*-methyl-D-aspartate (NMDA)-type subunit 2D (GRIN2D) in the amygdala⁹. AGIQ also increased the number of FOS-immunoreactive⁽⁺⁾ hippocampal granule cells. *Fos* is one of the immediate-early genes (IEGs) involved in the synaptic plasticity of hippocampal granule cells¹⁰. Moreover, GRIN2D is known to function in enhancing synaptic plasticity associated with long-term memory¹¹. These results suggest that the increases in FOS⁺ cells and *Grin2d* transcripts are associated with enhanced synaptic plasticity, which leads to the facilitation of fear extinction learning. Additionally, KIF21B was recently identified as a memory-rewriting molecule¹² that is found in the hippocampal dentate gyrus, which suggests a relationship with facilitation of fear memory extinction. However, in our previous study, changes were found in the constitutive levels of gene expression and numbers of immunoreactive cells in animals that were not subjected to behavioral tests. Thus, learning-mediated neuronal cellular responses require further elucidation.

Fear memory is regulated by an interplay among the hippocampus, prelimbic cortex, infralimbic cortex, and amygdala¹³. The hippocampus is an important region involved in the formation and storage of context memory in the fear conditioning test¹³. The prelimbic cortex and infralimbic cortex are subdivisions of the medial prefrontal cortex (mPFC) and accelerate and suppress fear expression, respectively¹³. The amygdala is critical for fear conditioning and fear extinction and modulates fear-related learning in other structures, such as the prelimbic cortex, infralimbic cortex, and hippocampus¹³. Memory formation is regulated by the synaptic plasticity of related neural circuits, and the degree of the changes in synaptic plasticity can be estimated by assessing IEG responses to various stimuli, such as during the learning test¹⁴. Therefore, the induction potential of synaptic plasticity-related IEGs that play roles in neuronal signal transmission—including glutamatergic receptors/transporters in the brain—may be directly related to the facilitation of fear extinction learning. In this sense, histopathological analysis of the IEG proteins in the brain regions regulating fear memory using immunohistochemistry may provide valuable information on the mechanism involved in AGIQ-induced facilitation of fear extinction learning. Specifically, the induction pattern of the IEG proteins after the last learning test trial may help to identify the brain regions responsible for strengthening neural circuits to facilitate fear extinction learning.

Recently, some polyphenolic antioxidants have been shown to exert an ameliorating effect on post-traumatic stress disorder (PTSD), a trauma and stressor-related disorder, in animal models^{15, 16}, and as a result, more attention has been given to these antioxidants. Surprisingly, a recent study has shown that dietary treatment with curcumin, a representative polyphenolic antioxidant, for 5 days impaired fear memory consolidation and reconsolidation processes in rats¹⁷. Because the sensitivity to exogenously administered antioxidants may vary among the different life stages, it is necessary to determine the optimum AGIQ exposure period for preventing or ameliorating anxiety. The present study evaluated different AGIQ exposure periods to identify the one that would be sufficient for facilitating fear extinction learning. We also examined the corresponding molecular responses in the brain regions involved in the facilitation. For these purposes, we examined the effects of AGIQ exposure in three different exposure periods: the postweaning exposure period, developmental exposure period, and entire developmental and postweaning exposure period. Behavioral tests were performed at both prepubertal and adult stages. In animals with whole period exposure to AGIQ, spontaneous recovery was also examined after the facilitation of fear extinction learning because preventing fear recovery is important for therapy related to anxiety disorders such as PTSD¹⁸. In animals subjected to spontaneous recovery, the number of immunoreactive cells for synaptic plasticity-related IEGs and their regulator, as well as constitutive changes in gene expression, in the brain regions of interest were compared among the different exposure periods. In animals that were subjected to whole period AGIQ exposure, similar immunohistochemistry and gene expression analyses were performed after the last trial of the learning test, and learning-linked responses were obtained for comparison with the changes in constitutive expression.

Materials and Methods

Chemicals and animals

AGIQ (purity: >97%) was provided by San-Ei Gen F.F.I., Inc. (Osaka, Japan). Thirty-six mated female Slc:SD rats at gestational day (GD) 1 (appearance of vaginal plugs was designated as GD 0) were purchased from Japan SLC, Inc. (Hamamatsu, Japan). Rats were individually housed with their offspring in polycarbonate cages with paper bedding until day 21 post-delivery. Animals were kept in an air-conditioned animal room (temperature: $23 \pm 2^\circ\text{C}$, relative humidity: $55 \pm 15\%$) with a 12-h light/dark cycle and provided powdered basal diet (CRF-1; Oriental Yeast Co., Ltd., Tokyo, Japan) *ad libitum* until exposure to AGIQ began and tap water *ad libitum* during the experiment. Offspring were weaned at postnatal day (PND) 21 (where PND 0 was the day of delivery) and reared two animals per cage thereafter and provided powdered basal diet with or without AGIQ and tap water *ad libitum*.

Experimental design

Mated female rats were randomly divided into two groups of untreated controls (18 animals) and the AGIQ group (18 animals) (Fig. 1). Animals in the AGIQ group were administered 0.5% AGIQ (w/w) in their powdered basal diet from GD 6 to day 21 post-delivery. The dosage we chose has been shown to facilitate fear extinction learning with continuous exposure from fetal stages to adulthood⁹.

We measured the body weight (BW) and food and water consumption of the dams every 3–4 days from GD 6 to day 21 post-delivery. On PND 4, litters were randomly culled to preserve 6 or 7 male and 1 or 2 female offspring per dam (a total of 8 offspring per dam). The offspring were weighed every 3 or 4 days until PND 21. Dams and female offspring were euthanized by exsanguination through the abdominal aorta under CO₂/O₂ anesthesia on day 22 post-delivery. Male offspring were selected for behavioral tests and immunohistochemical and gene expression analyses because animal behaviors are influenced by circulating levels of steroid hormones during the estrous cycle^{19–21}. From PND 21, the remaining male offspring in the untreated controls and AGIQ group were left untreated or dietarily exposed to AGIQ, respectively. On PND 30, animals that had been subjected to prepubertal behavioral tests were subjected to brain sampling for other experimental purposes.

From PND 30 onwards, the remaining male offspring from both groups were either left untreated or exposed to AGIQ. There were four animal groups: untreated controls (Ctrl; 32 animals), the postweaning AGIQ-exposed group (PW-AGIQ; 32 animals), the developmental AGIQ-exposed group (DEV-AGIQ; 32 animals), and the whole period AGIQ-exposed group (WP-AGIQ; 32 animals) (Fig. 1). Offspring in the PW-AGIQ and WP-AGIQ groups were fed a

powdered diet containing 0.5% AGIQ *ad libitum*. Rats in all groups were weighed once weekly thereafter, and the amounts of food and water consumed were also recorded.

On PND 76 and PND 79, animals were subjected to brain sampling after the end of the adult stage behavioral tests (adult stage test 1, PND 76; adult stage test 2, PND 79). For brain immunohistochemistry, 10 male offspring per group (1 pup per dam) were subjected to perfusion fixation through the left cardiac ventricle with ice-cold 4% (w/v) paraformaldehyde (PFA) in 0.1 M phosphate buffer (pH 7.4) at a flow rate of 35 mL/min under deep CO₂/O₂-induced anesthesia. For gene expression analysis, 6 male offspring per group (1 pup per dam) were euthanized by exsanguination through the abdominal aorta under CO₂/O₂ anesthesia and subjected to necropsy. The brains were removed and then fixed in methacarn solution at 4°C for 5 h.

All dams and offspring were checked each day to assess their general appearance (abnormal gait and behaviors). All procedures in this study were conducted in accordance with the National Institutes of Health Guide for the Care and Use of Laboratory Animals (NIH Publications No. 8023, revised 1978) and according to the protocol approved by the Animal Care and Use Committee of The Tokyo University of Agriculture and Technology (Approved No.: 29-82). All efforts were made to minimize animal suffering.

Behavioral tests

Animals included in the prepubertal stage test (untreated controls and the AGIQ group) and adult stage test 1 (untreated controls and the DEV-AGIQ, PW-AGIQ, and WP-AGIQ groups) were subjected to the open field test, object recognition test, and contextual fear conditioning test. Animals included in adult stage test 1 also completed the

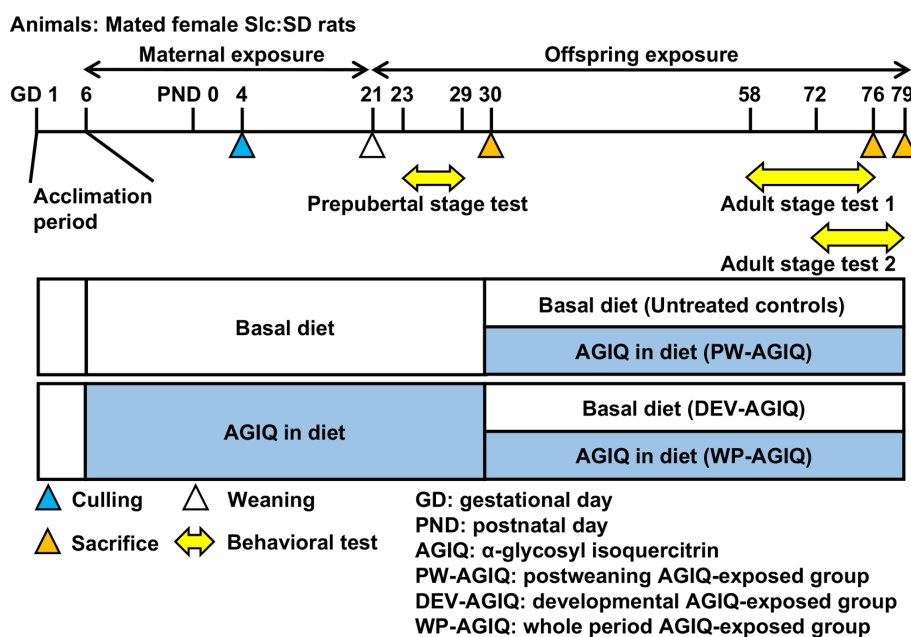


Fig. 1. Experimental design for continuous exposure to α-glycosyl isoquercitrin (AGIQ) from fetal stages to adulthood in rats.

spontaneous recovery test. Animals included in adult stage test 2 (untreated controls and the WP-AGIQ group) were subjected to the contextual fear conditioning test.

In each behavior experiment, animals were transported from the animal room to the behavioral test room 1–2 h before starting the tests. After the end of each behavioral test, animals were promptly returned to their home cage and transferred to the animal room. Apparatuses were cleaned with 70% ethanol solution before and after each test. All experiments were conducted between 08:00 and 19:00, and the order of animal selection for tests among groups was counter-balanced across the test time to avoid any bias resulting from the trial times of each group.

Open field test

The open field test was performed on PND 23 and PND 24 (prepubertal stage test) and on PND 58 and PND 61 (adult stage test 1) to assess locomotor activity and anxiety-like behaviors and to habituate the rats to the arena that would be used in the object recognition test on the following day (acclimation phase). The arena comprised a square stainless-steel tray with a matte black polyvinyl plastic surface and stainless-steel walls surrounding a tray with a matte black polyvinyl plastic surface (900 mm width × 900 mm depth × 500 mm height, O'Hara & Co., Ltd., Tokyo, Japan). The illumination was set at 20 Lux at the middle of the arena. The animals were placed at the corner of the arena with their heads facing the wall and allowed to explore the arena freely for 10 min. The total distance and time spent in the center or peripheral areas of the field were recorded by a CCD camera (WAT-902B; Watec Co., Ltd., Tsuruoka, Japan) mounted above the arena and evaluated by an automatic video-tracking system (TimeOFCR1 software; O'Hara & Co., Ltd.). In the video tracking analysis, the field was divided equally into 25 square regions, and 9 central regions were defined as the center area. The percentage of time spent in the center area was calculated. The center area rate was defined as the percentage of time that an animal stayed in the center area during the observation time.

Object recognition test

The object recognition test was performed on PND 24 and PND 25 (prepubertal stage test) and on PND 59 to PND 62 (adult stage test 1) to assess object recognition memory. Experiments were conducted in the same arena that was used in the open field test. The test comprised three steps: acclimation, sample phase, and test phase. Twenty-four hours after acclimation, the animals were allowed to explore the arena for 5 min with two identical sample objects (sample phase). After a prescribed interval (1 or 4 h for the prepubertal stage test or 1 or 24 h for adult stage test 1), the animals were allowed to explore the arena for 3 min with one familiar sample object and one novel object (test phase). In the sample and test phases, the animals were placed in the middle of the wall along the inside of the field with their heads facing the wall. Objects were placed equidistant to this location to the right and left sides behind the animal in

the arena. The illumination was set at 20 Lux at the middle of the arena. The sample object was a black and white striped quadrangular prism with smooth polyvinyl plastic surfaces. The novel object was a gray cone of polyvinyl plastic with a rough surface and a stainless-steel tip. These objects were heavy enough that they could not be moved by the animals. Animal behavior was recorded by a CCD camera (WAT-902B; Watec Co., Ltd.) mounted above the arena and evaluated by an automatic video-tracking system (TimeSSI software; O'Hara & Co., Ltd.). Total distance and exploration time toward each object were recorded. When a rat's nose approached to within 3 cm of an object, the video-tracking system automatically counted it as "exploration," and the cumulative exploration time was recorded. In the test phase, animal behavior was analyzed during the first 2 min because the novel object becomes increasingly familiar and exploration time decreases as time passes. A discrimination index for novel object recognition was determined using following formula:

$$\text{Discrimination index} = \frac{\text{exploration time with novel object}}{\text{exploration time with familiar object} + \text{exploration time with novel object}}$$

Contextual fear conditioning test

The contextual fear conditioning test was performed on PND 26 to PND 29 (prepubertal stage test), PND 65 to PND 76 (adult stage test 1), and PND 71 to PND 79 (adult stage test 2) (Fig. 2, Supplementary Fig. 1: online only).

Conditioning and testing took place in a rodent observation cage (30 × 37 × 25 cm; CL-3001; O'Hara & Co., Ltd.) that was placed in a sound-attenuating chamber (CL-4211; O'Hara & Co., Ltd.). The side walls and door of the observation cage were constructed of Plexiglas. The floor comprised 21 steel rods through which a scrambled footshock from a shock generator (SGA-2020; O'Hara & Co., Ltd.) could be delivered. During experiments, the chamber was ventilated, kept at a background white noise level of 50 dB, and illuminated at 200 Lux by white light-emitting diode bulbs. Animal behavior was video recorded by a CCD camera (WAT-902B; Watec Co., Ltd.) and analyzed using an automatic video-tracking system (TimeFZ2 software; O'Hara & Co., Ltd.). Body freezing time was measured, and the freezing rate was defined as the percentage of time that the animal was immobile during the test.

Contextual fear conditioning: 138 s after transferring the animals to the cage, they received two 2-s footshocks (0.5 mA intensity) 100 s apart. The animals were removed from the cage 60 s after the second footshock and returned to their home cages. Thus, fear conditioning took 5 min.

Fear acquisition, fear extinction, and spontaneous recovery: Animals were placed back in the same context as used for conditioning for 5 min without footshock. Ninety minutes after completion of adult stage tests 1 and 2 (the spontaneous recovery test or the fear extinction test), the animals were euthanized for immunohistochemistry and real-time reverse transcription PCR analysis of the brain.

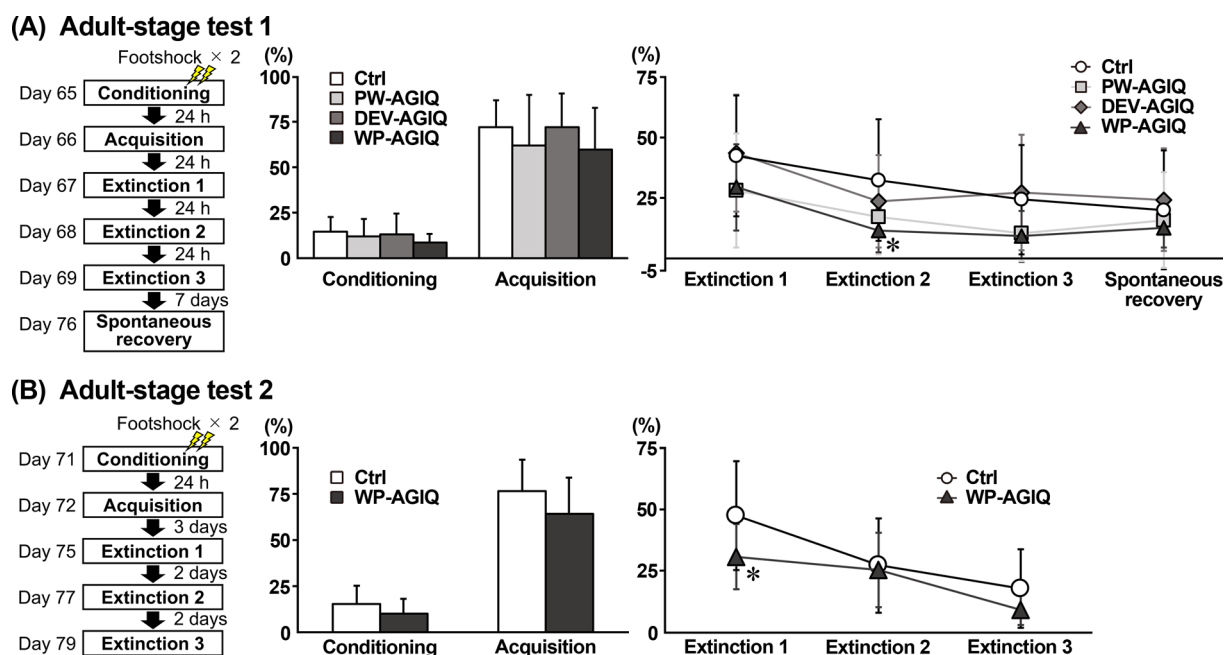


Fig. 2. Experimental design of the contextual fear conditioning test and freezing rate (%) during the fear conditioning, fear acquisition, fear extinction, and spontaneous recovery tests in the untreated controls and each α -glycosyl isoquercitrin (AGIQ)-exposed group at adult stage tests 1 and 2. (A) Adult stage test 1. (B) Adult stage test 2. Values are expressed as the mean + SD or mean \pm SD. $n = 13$ – 16 /group for adult stage test 1 (conditioning and acquisition: untreated controls (Ctrl), 16; postweaning AGIQ-exposed group (PW-AGIQ), 16; developmental AGIQ-exposed group (DEV-AGIQ), 16; whole period AGIQ-exposed group (WP-AGIQ), 16; fear extinction 1–3 and spontaneous recovery: Ctrl, 16; PW-AGIQ, 14; DEV-AGIQ, 16; WP-AGIQ, 13). $n = 14$ – 16 /group for adult stage test 2 (conditioning and acquisition: Ctrl, 16; WP-AGIQ, 16; fear extinction 1–3: Ctrl, 16; WP-AGIQ, 14). * $P < 0.05$, significantly different from the untreated controls by Dunnett's test or Aspin-Welch's t -test with Bonferroni correction (adult stage test 1) or significantly different from the untreated controls by Student's t -test or Aspin-Welch's t -test (adult stage test 2).

Immunohistochemistry

Because IEG peak protein expression in response to acute stimuli occurs within approximately 90–120 min²², animals were euthanized for perfusion fixation 90 min after the last trial of the contextual fear conditioning test. Perfusion-fixed brains were additionally fixed with the same PFA buffer solution overnight. Coronal slices were prepared at +3.0 mm and –3.0 mm from the bregma after adult stage tests 1 and 2 ($n = 10$ /group). For immunohistochemistry of the hippocampal dentate gyrus and amygdala, a 3 mm-thick slice posterior to the –3.0 mm coronal plane from the bregma was prepared. For immunohistochemistry of the prelimbic and infralimbic cortices, a 3 mm-thick slice anterior to the +2.0 mm coronal plane from the bregma was prepared. Brain slices were further fixed with the same PFA buffer solution overnight at 4°C and routinely processed for paraffin embedding and sliced into 3- μ m-thick sections.

Brain sections were subjected to immunohistochemical analysis using primary antibodies against the following: activity-regulated cytoskeleton-associated protein (ARC), FOS, early growth response 1 (EGR1), and cyclooxygenase 2 (COX2), which are IEGs involved in synaptic plasticity^{10, 23}, and phosphorylated extracellular signal-regulated kinase 1/2 (p-ERK1/2), a member of the mitogen activated protein kinase (MAPK) family that is activated by phos-

phorylation to promote transcriptional programs leading to the induction of *Arc* and *Fos*²⁴. To block endogenous peroxidase, deparaffinized sections were incubated in 0.3% (v/v) H₂O₂ solution in absolute methanol for 30 min. The antigen retrieval conditions that were applied for some antibodies are listed in Supplementary Table 1 (online only). Immunodetection was conducted using a Vectastain® *Elite* ABC kit (PK-6101 and PK-6102; Vector Laboratories Inc., Burlingame, CA, USA) with 3,3'-diaminobenzidine/H₂O₂ as the chromogen. Hematoxylin counterstaining was then performed, and coverslips were mounted on immunostained sections for microscopic examination.

Evaluation of immunoreactive cells

Immunoreactive cells (ARC⁺, COX2⁺, EGR1⁺, FOS⁺, and p-ERK1/2⁺ cells) in the hippocampal granule cell layer (GCL) were bilaterally counted and normalized for the length of the subgranular zone of the dentate gyrus (Supplementary Fig. 2: online only). Immunoreactive cells distributed within the prelimbic cortex, infralimbic cortex, lateral amygdala, basolateral amygdala, and central nucleus of the amygdala were bilaterally counted and normalized per area unit (Supplementary Fig. 3 and 4: online only). Number of each immunoreactive cellular population was manually counted under microscopic observation using a BX53 microscope (Olympus Corporation, Tokyo, Japan). The posi-

tion and shape of each area were determined with reference to cresyl violet staining images adjacent to the immunostained section and the atlas of the rat brain²⁵. Immunolocalized cells were analyzed while blinded to the treatment conditions. The length of the subgranular zone of the dentate gyrus and the area of the prelimbic cortex, infralimbic cortex, lateral amygdala, basolateral amygdala, and central nucleus of the amygdala were measured and determined based on microscopic images at $\times 25$ -fold or $\times 40$ -fold magnification by applying the cellSens Standard (version 1.9; Olympus Corp., Tokyo, Japan).

Transcript-level expression analysis

To analyze gene expression, transcript levels in the hippocampal dentate gyrus, prelimbic cortex, infralimbic cortex, and amygdala were examined after adult stage tests 1 and 2 using real-time RT-PCR. Tissues were dissected according to the whole-brain fixation method using methacarn solution as previously reported²⁶. In brief, a 2 mm-thick slice posterior to the -2.0 mm coronal plane from the bregma was prepared to collect tissue samples from the hippocampal dentate gyrus and amygdala using a punch biopsy device with a pore-size diameter of 1 mm (BP-10F; Kai Industries Co., Ltd., Gifu, Japan). For sampling the infralimbic cortex and prelimbic cortex tissues, a 2-mm coronal-thick slice anterior to the $+2.0$ mm coronal plane from the bregma was prepared (Supplementary Fig. 5: online only). Total RNA was extracted from brain tissue samples from all groups ($n = 6$ per group) using RNeasy Mini kits (Qiagen, Hilden, Germany). First-strand cDNA was synthesized using SuperScript[®] III Reverse Transcriptase (Thermo Fisher Scientific, Waltham, MA, USA) in a 20- μ L total reaction mixture with 1 μ g of total RNA. Analysis of the transcript levels for the gene targets shown in Supplementary Table 2 (online only) was performed using PCR primers designed with Primer Express software (Version 3.0; Thermo Fisher Scientific). Real-time PCR with Power SYBR[®] Green PCR Master Mix (Thermo Fisher Scientific) was conducted using a StepOnePlus[™] Real-time PCR System (Thermo Fisher Scientific). The relative differences in gene expression between the untreated controls and each treatment group were calculated using threshold cycle (C_T) values that were first normalized to that of hypoxanthine phosphoribosyltransferase 1 (*Hprt1*) or glyceraldehyde-3-phosphate dehydrogenase (*Gapdh*), which served as endogenous controls in the same sample, and then relative to a control C_T value using the $2^{-\Delta\Delta C_T}$ method²⁷.

Statistical analysis

Offspring data from PND 30 onwards (BW and brain weight at necropsy, scores on the behavioral tests, number of immunoreactive cells for each antigen, and results from the transcript-level gene-expression analysis) were analyzed using the individual animals as the experimental unit. Data from 4 groups were analyzed using Levene's test for homogeneity of variance. If the variance was homogenous, numerical data were evaluated using Dunnett's test for com-

parisons between the untreated controls and each treatment group. For heterogeneous data, Aspin-Welch's *t*-test with Bonferroni correction was used. Data from two groups were analyzed using the Levene's test for homogeneity of variance. When the variance was homogenous, Student's *t*-test was applied. When data were heterogeneous, Aspin-Welch's *t*-test was used. All analyses were performed using IBM SPSS Statistics ver. 25 (IBM Corp., Armonk, NY, USA), and $P < 0.05$ was considered statistically significant.

Because some animals were resistant to fear extinction learning, the Smirnov-Grubbs test was performed to detect the outliers in each group. Identified outliers were excluded as abnormal animals from the fear extinction test analysis, spontaneous recovery test analysis, immunohistochemistry analysis, and transcript-level gene-expression analysis. The Smirnov-Grubbs test was performed using Excel Statistics 2013 software package version 2.02 (Social Survey Research Information Co. Ltd., Tokyo, Japan), and $P < 0.05$ was considered statistically significant.

Results

Maternal parameters

One non-pregnant animal in the AGIQ group was excluded from the experiment. Therefore, the effective numbers of dams in the untreated controls and AGIQ group were 18 and 17, respectively. Based on the mean food consumption values, dams in the AGIQ group received 333.9 and 656.5 mg/kg BW/day AGIQ during the gestation and lactation periods, respectively.

Offspring necropsy data

The AGIQ group at necropsy on PND 30 and the PW-AGIQ, DEV-AGIQ, and WP-AGIQ groups at necropsies on PND 76 or PND 79 showed no significant differences in BW and absolute and relative brain weights compared with the untreated controls (Supplementary Table 3 and 4: online only). Based on the mean food consumption values, offspring received 693.9 mg/kg BW/day AGIQ between PND 21 and PND 30. Thereafter, offspring in the PW-AGIQ and WP-AGIQ groups received 415.7 and 425.4 mg/kg BW/day AGIQ, respectively.

Behavioral testing scores of male offspring

Open field test: In the prepubertal stage test, there were no significant differences in the total distance and center area rate between the untreated controls and AGIQ group (Supplementary Table 5: online only).

In adult stage test 1, there were no significant differences in the total distance and center area rate between the untreated controls and any of the AGIQ groups (Supplementary Table 6: online only).

Object recognition test: In the prepubertal stage test, there were no significant differences in the total distance and discrimination index in the test phase after 1 h and 4 h intervals between the untreated controls and AGIQ group (Supplementary Table 7: online only).

In adult stage test 1, there were no significant differences in the total distance and discrimination index in the test phase after 24 h and 1 h interval between the untreated controls and any of the AGIQ groups (Supplementary Table 8: online only).

Contextual fear conditioning test: In the prepubertal stage test, there were no significant differences in the freezing rate in the fear acquisition and fear extinction tests between the untreated controls and AGIQ group (Supplementary Table 9: online only).

In adult stage test 1, the WP-AGIQ group showed a significantly lower freezing rate in the 2nd trial of the fear extinction test than the untreated controls, while the freezing rate in the PW-AGIQ and DEV-AGIQ groups did not differ from that of the untreated controls (Fig. 2, Supplementary Table 10: online only). There were no significant changes in the spontaneous recovery test between the untreated controls and any of the AGIQ groups.

In adult stage test 2, the WP-AGIQ group showed a significantly lower freezing rate in the 1st trial of the fear extinction test than the untreated controls (Fig. 2, Supplementary Table 11: online only).

Number of immunoreactive cells for synaptic plasticity-related IEGs and their regulator

GCL of the hippocampal dentate gyrus: In adult stage test 1, there were no significant differences in the number of immunoreactive cells for any molecule in the GCL between the untreated controls and any of the AGIQ groups (Supplementary Fig. 6: online only, Table 1).

In adult stage test 2, there were no significant differences in the number of immunoreactive cells for any molecule in the GCL between the untreated controls and WP-AGIQ group (Fig. 3, Table 2).

mPFC: In adult stage test 1, there were no significant differences in the number of immunoreactive cells for any molecule in the prelimbic cortex between the untreated controls and any of the AGIQ groups (Supplementary Fig. 7: online only, Table 1). The number of FOS⁺ cells in the infralimbic cortex significantly increased in the WP-AGIQ group compared with that in the untreated controls (Supplementary Fig. 8: online only, Table 1). No significant differences in the number of immunoreactive cells for other molecules in the infralimbic cortex were observed between the untreated controls and any of the AGIQ groups.

In adult stage test 2, the number of p-ERK1/2⁺ cells in the prelimbic cortex significantly increased in the WP-AGIQ group compared with that in the untreated controls

Table 1. Number of Immunoreactive Cells in the Granule Cell Layer of the Hippocampal Dentate Gyrus, Prelimbic Cortex, and Infralimbic Cortex of Male Offspring after Adult Stage Test 1

	Ctrl	PW-AGIQ	DEV-AGIQ	WP-AGIQ
No. of offspring examined	10	10 (8) [†]	10	10 (7) [‡]
Hippocampal dentate gyrus				
Granule cell layer (No./mm ²)				
ARC	3.9 ± 1.7	3.9 ± 1.7	3.4 ± 1.7	5.1 ± 1.5
COX2	4.4 ± 2.3	6.8 ± 2.9	3.8 ± 1.8	3.0 ± 1.1
EGR1	4.6 ± 2.4	5.2 ± 3.1	4.3 ± 1.9	5.0 ± 1.7
FOS	3.2 ± 1.1	3.6 ± 1.8	2.9 ± 1.6	4.1 ± 2.0
p-ERK1/2	1.1 ± 0.7	0.6 ± 0.4	1.0 ± 0.8	0.8 ± 0.7
Medial prefrontal cortex				
Prelimbic cortex (No./mm ²)				
ARC	1.0 ± 1.1	1.0 ± 1.0	1.4 ± 1.6	1.2 ± 0.8
COX2	10.4 ± 5.0	11.0 ± 7.1	27.9 ± 23.6	17.4 ± 8.1
EGR1	247.4 ± 109.1	222.0 ± 110.8	202.1 ± 73.0	253.9 ± 122.3
FOS	27.4 ± 13.3	30.8 ± 14.5	28.1 ± 13.1	33.7 ± 15.4
p-ERK1/2	39.7 ± 13.7	39.9 ± 29.6	39.7 ± 16.3	55.6 ± 22.2
Infralimbic cortex (No./mm ²)				
ARC	0.3 ± 0.4	0.7 ± 1.1	1.4 ± 2.1	0.1 ± 0.3
COX2	5.3 ± 3.9	5.2 ± 2.2	11.2 ± 6.5	11.5 ± 7.1
EGR1	123.0 ± 62.0	116.0 ± 60.7	131.2 ± 42.9	140.1 ± 69.0
FOS	16.1 ± 7.3	23.0 ± 13.2	20.1 ± 11.3	31.1 ± 14.8*
p-ERK1/2	76.0 ± 26.0	68.2 ± 26.6	61.8 ± 23.1	85.1 ± 32.3

AGIQ, α -glycosyl isoquercitrin; ARC, activity-regulated cytoskeleton-associated protein; COX2, cyclooxygenase 2; Ctrl, untreated controls; DEV-AGIQ, developmental AGIQ-exposed group; EGR1, early growth response 1; FOS, Fos proto-oncogene, AP-1 transcription factor subunit; p-ERK1/2, phospho-extracellular signal-regulated kinase 1/2; PW-AGIQ, postweaning AGIQ-exposed group; WP-AGIQ, whole-period AGIQ-exposed group. Data are expressed as mean \pm SD. * $P < 0.05$, significantly different from the untreated controls by Dunnett's test or Aspin-Welch's *t*-test with Bonferroni correction. [†]Two animals that were detected as fear-extinction outliers by the Smirnov-Grubbs test were excluded from data analysis. The number in parenthesis is the effective number of animals. [‡]Three animals that were detected as fear-extinction outliers by the Smirnov-Grubbs test were excluded from data analysis. The number in parenthesis is the effective number of animals.

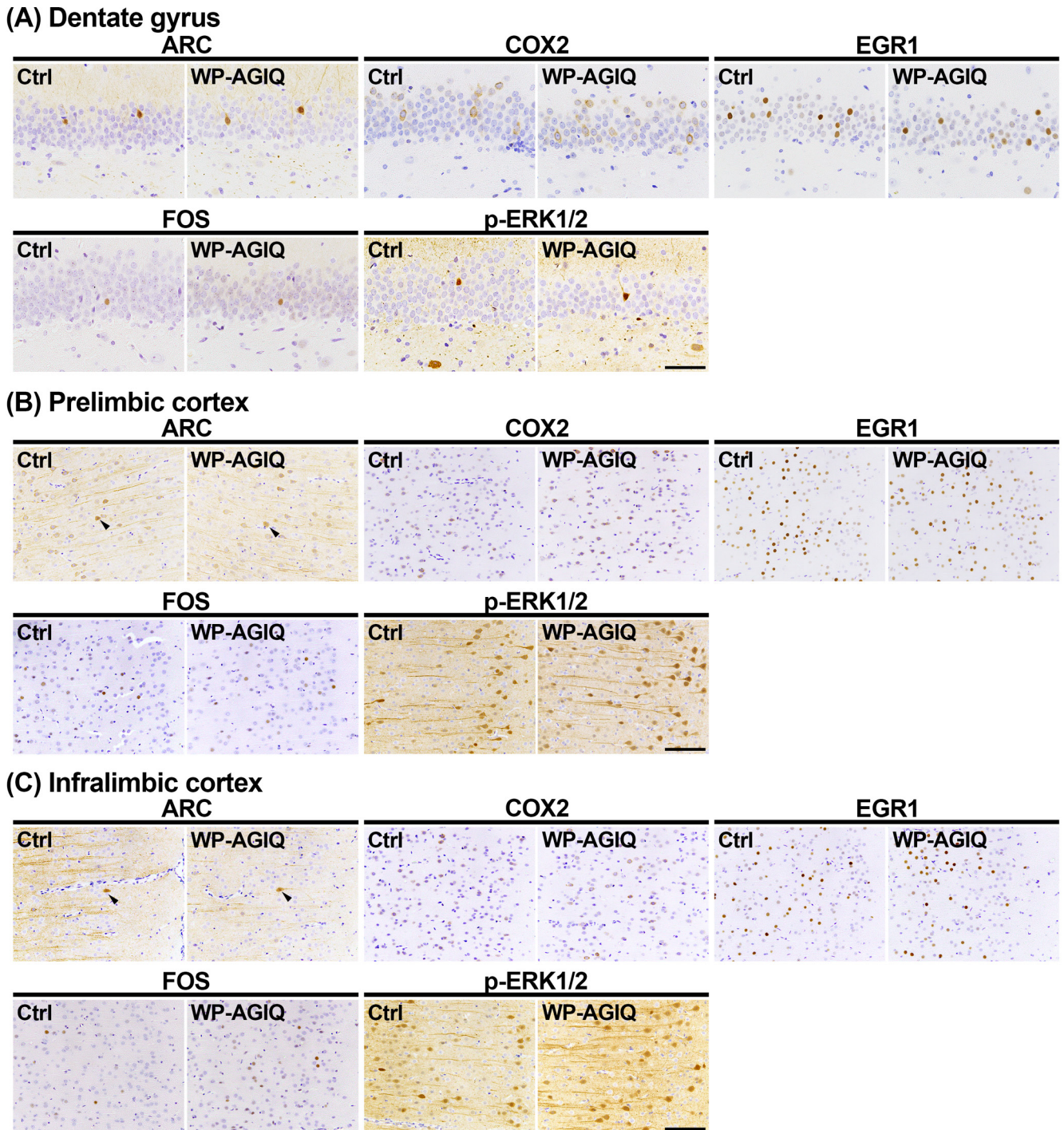


Fig. 3. Distribution of immunoreactive cells for activity-regulated cytoskeleton associated protein (ARC), cyclooxygenase 2 (COX2), early growth response 1 (EGR1), Fos proto-oncogene, AP-1 transcription factor subunit (FOS), and phosphorylated extracellular signal-regulated kinase 1/2 (p-ERK1/2) in the respective brain regions of a male offspring after the last trial of the fear extinction test at adult stage test 2. (A) Granule cell layer (GCL) of the hippocampal dentate gyrus. (B) Prelimbic cortex. (C) Infralimbic cortex. Representative images from the untreated controls (Ctrl; left) and whole period AGIQ-exposed group (WP-AGIQ; right) rats. Arrowheads indicate immunoreactive cells. Magnifications: (A) $\times 400$; bar, 50 μm . (B) and (C) $\times 200$; bar, 100 μm .

(Fig. 3, Table 2). No significant differences in the number of immunoreactive cells for other molecules in the prelimbic cortex were observed between the WP-AGIQ group and untreated controls (Fig. 3, Table 2). The numbers of FOS⁺

and p-ERK1/2⁺ cells in the infralimbic cortex significantly increased in the WP-AGIQ group compared with those in the untreated controls (Fig. 3, Table 2). There were no significant differences in the number of immunoreactive cells

Table 2. Number of Immunoreactive Cells in the Granule Cell Layer of the Hippocampal Dentate Gyrus, Prelimbic Cortex, Infralimbic Cortex, Lateral Amygdala, Basolateral Amygdala, and Central Nucleus of the Amygdala of Male Offspring after Adult Stage Test 2

	Ctrl	WP-AGIQ
No. of offspring examined	10	10
Hippocampal dentate gyrus		
Granule cell layer (No./mm)		
ARC	3.3 ± 1.2	4.2 ± 1.2
COX2	17.5 ± 6.2	18.5 ± 6.5
EGR1	16.9 ± 5.8	18.1 ± 4.2
FOS	1.7 ± 1.0	1.6 ± 0.7
p-ERK1/2	1.1 ± 1.0	1.1 ± 0.4
Medial prefrontal cortex		
Prelimbic cortex (No./mm ²)		
ARC	4.5 ± 3.7	7.5 ± 5.8
COX2	20.7 ± 14.2	37.2 ± 21.1
EGR1	182.8 ± 80.7	182.2 ± 40.0
FOS	14.9 ± 8.0	17.5 ± 11.1
p-ERK1/2	28.6 ± 16.0	58.4 ± 20.3*
Infralimbic cortex (No./mm ²)		
ARC	2.8 ± 2.9	5.2 ± 3.8
COX2	11.8 ± 9.0	12.1 ± 5.9
EGR1	87.3 ± 44.6	107.2 ± 34.5
FOS	13.9 ± 7.7	24.0 ± 12.2*
p-ERK1/2	52.7 ± 17.3	79.1 ± 23.2*
Amygdala		
Lateral amygdala (No./mm ²)		
ARC	0 ± 0	0.3 ± 0.7
COX2	27.9 ± 20.4	49.5 ± 38.6
EGR1	297.1 ± 168.0	331.5 ± 129.2
FOS	12.0 ± 14.7	34.4 ± 43.5
p-ERK1/2	6.5 ± 8.5	16.2 ± 20.5
Basolateral amygdala (No./mm ²)		
ARC	0 ± 0	0.1 ± 0.4
COX2	2.0 ± 1.6	1.8 ± 1.8
EGR1	196.5 ± 70.2	193.6 ± 38.6
FOS	18.3 ± 15.7	26.4 ± 28.9
p-ERK1/2	8.4 ± 8.9	16.6 ± 21.8
Central nucleus of amygdala (No./mm ²)		
ARC	0.2 ± 0.7	0 ± 0
COX2	0.6 ± 1.7	0 ± 0
EGR1	95.4 ± 74.8	104.2 ± 60.1
FOS	23.8 ± 26.4	17.2 ± 24.3
p-ERK1/2	2.3 ± 3.2	1.0 ± 1.6

AGIQ, α -glycosyl isoquercitrin; ARC, activity-regulated cytoskeleton-associated protein; COX2, cyclooxygenase 2; Ctrl, untreated controls; EGR1, early growth response 1; FOS, Fos proto-oncogene, AP-1 transcription factor subunit; p-ERK1/2, phospho-extracellular signal-regulated kinase 1/2; WP-AGIQ, whole-period AGIQ-exposed group. Data are expressed as mean \pm SD. * P <0.05, significantly different from the untreated controls by Student's *t*-test or Aspin-Welch's *t*-test.

for other molecules in the infralimbic cortex between the untreated controls and WP-AGIQ group (Fig. 3, Table 2).

Amygdala: There were either no or a few ARC⁺ cells in the lateral amygdala, basolateral amygdala, and central nucleus of the amygdala and either no or a few COX2⁺ cells in the basolateral amygdala and central nucleus of the amygdala. In adult stage test 2, there were no significant differences in the number of immunoreactive cells for any molecule in the lateral amygdala, basolateral amygdala, and

central nucleus of the amygdala between the untreated controls and WP-AGIQ group (Fig. 4, Table 2).

Transcript-level expression changes

Hippocampal dentate gyrus: In adult stage test 1, there were no changes in transcript levels in the PW-AGIQ group compared with the untreated controls (Fig. 5, Supplementary Table 12: online only). In the DEV-AGIQ group, compared with the levels in the untreated controls, the transcript

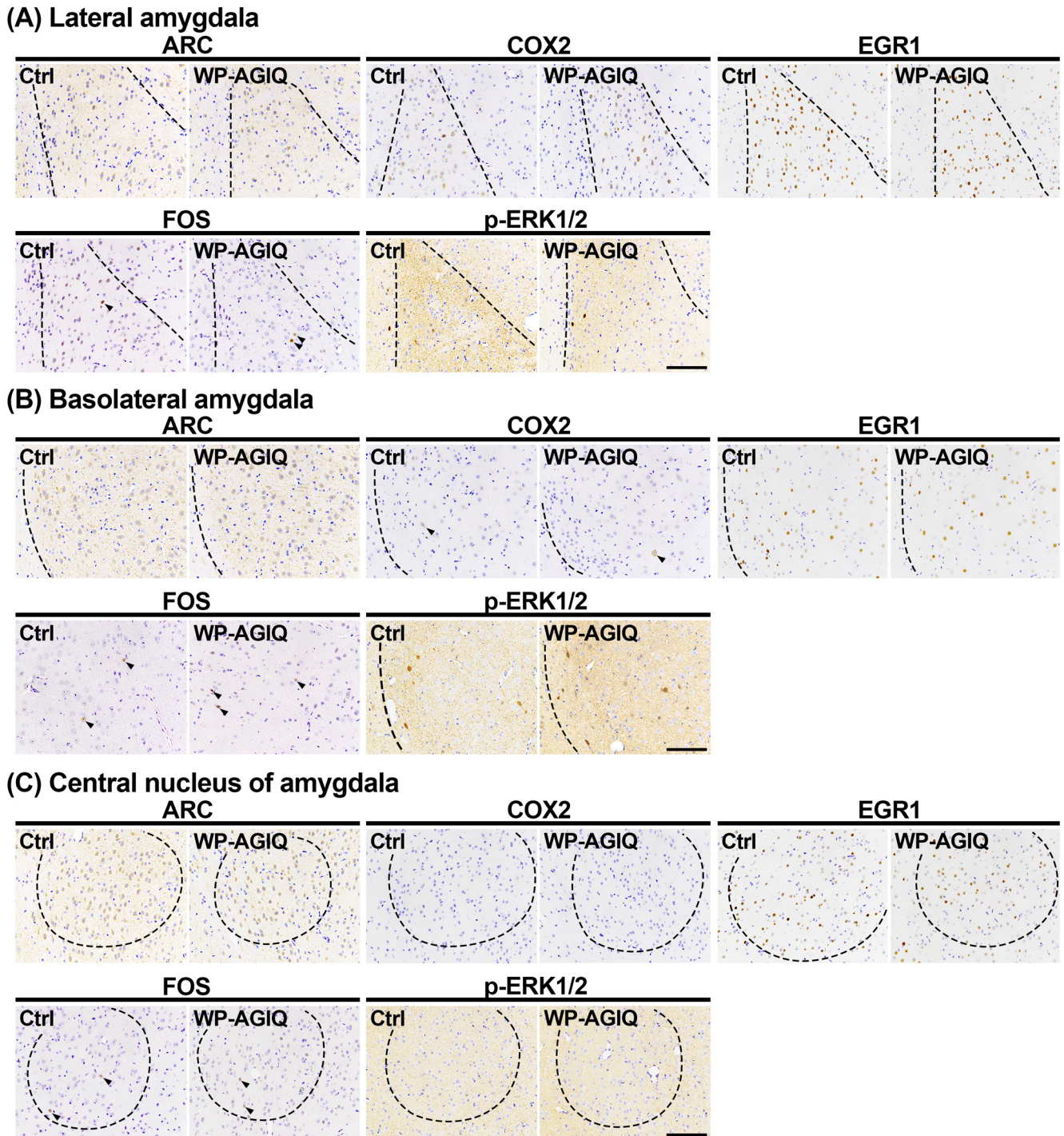


Fig. 4. Distribution of immunoreactive cells for activity-regulated cytoskeleton associated protein (ARC), cyclooxygenase 2 (COX2), early growth response 1 (EGR1), Fos proto-oncogene, AP-1 transcription factor subunit (FOS), and phosphorylated extracellular signal-regulated kinase 1/2 (p-ERK1/2) in subregions of the amygdala of a male offspring after the last trial of the fear extinction test at adult stage test 2. (A) Lateral amygdala. (B) Basolateral amygdala. (C) Central nucleus of the amygdala. Representative images from the untreated controls (Ctrl; left) and whole period AGIQ-exposed group (WP-AGIQ; right) rats. Arrowheads indicate immunoreactive cells. Magnification, $\times 200$; bar, 100 μm .

levels of *Grin2c*, *Slc17a6*, *Fos*, *Flt1*, *Kdr*, *Vegfa*, *Pcna*, *Nos3*, and *Elmo1* were significantly increased, while the transcript levels of *Efnb3*, *Epha4*, *Ephb2*, *Grial*, *Gria2*, *Gria3*, *Grin2a*, *Grin2b*, *Slc17a7*, *Bdnf*, *Arc*, *Egr1*, *Mapk1*, *Ptgs2*, and

Nos1 were significantly decreased after normalization with *Gapdh* and/or *Hprt1*. In the WP-AGIQ group, compared with the levels in the untreated controls, the transcript levels of *Ephb1*, *Fos*, *Flt1*, *Kdr*, *Notch1*, *Vegfa*, *Pcna*, *Nos2*, *Nos3*,

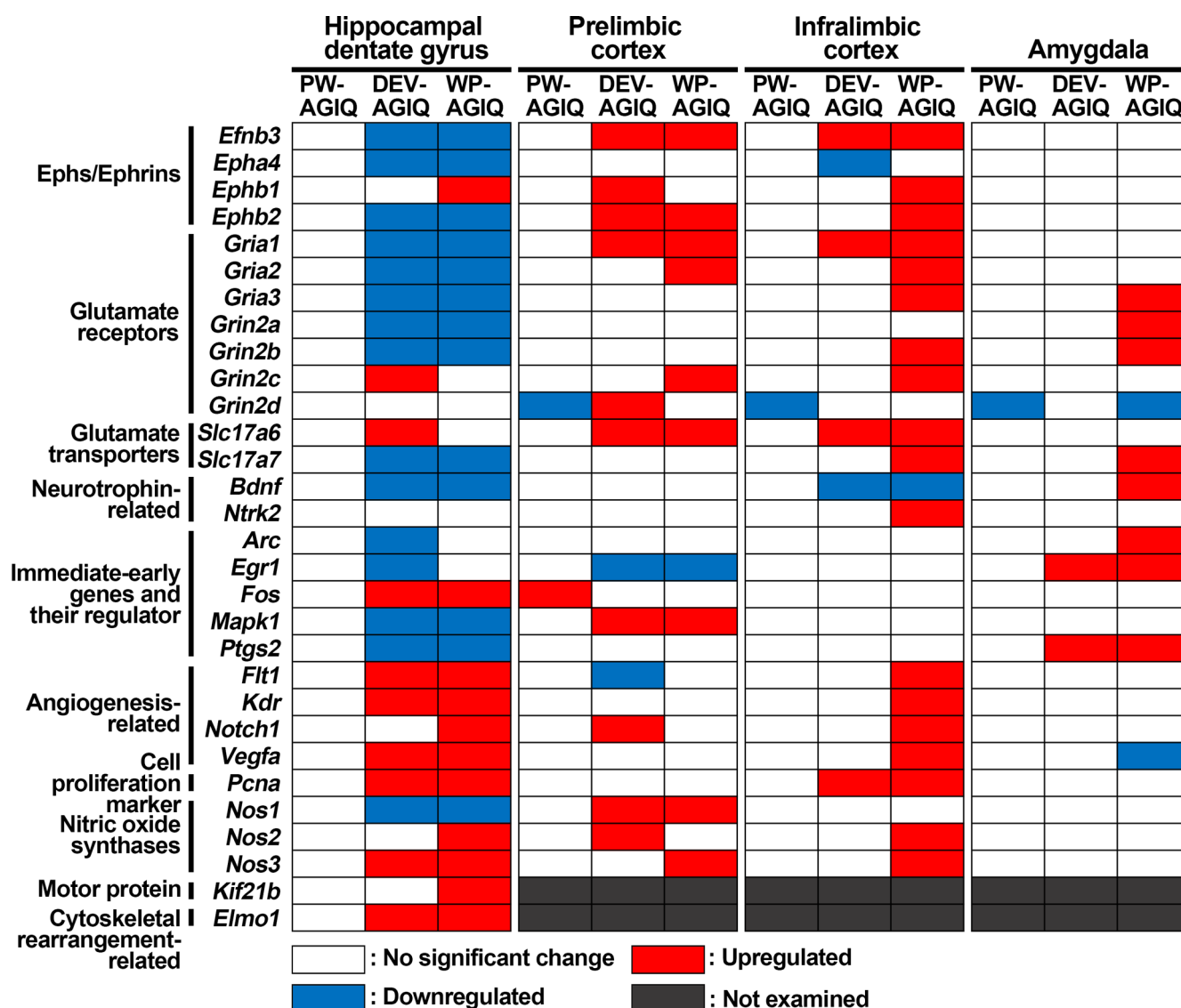


Fig. 5. Summary of the changes in gene expression in specified brain regions after adult stage test 1. Genes with higher or lower transcript levels than those in the untreated controls after normalization with either or both glyceraldehyde-3-phosphate dehydrogenase (*Gapdh*) and hypoxanthine phosphoribosyltransferase 1 (*Hprt1*) were judged to be upregulated or downregulated, respectively.

Kif21b, and *Elmo1* were significantly increased, while the transcript levels of *Efnb3*, *Epha4*, *Ephb2*, *Gria1*, *Gria2*, *Gria3*, *Grin2a*, *Grin2b*, *Slc17a7*, *Bdnf*, *Mapk1*, *Ptgs2*, and *Nos1* were significantly decreased after normalization with *Gapdh* and/or *Hprt1*.

In adult stage test 2, the transcript levels of *Efnb3*, *Epha4*, *Ephb2*, *Gria1*, *Gria2*, *Gria3*, *Grin2a*, *Grin2b*, *Grin2c*, *Slc17a7*, *Egr1*, *Mapk1*, and *Kif21b* were significantly increased after normalization with *Gapdh* and/or *Hprt1* in the WP-AGIQ group compared with the levels in the untreated controls (Supplementary Table 13: online only). The transcript level of *Grin2d* was significantly decreased after normalization with *Gapdh* and *Hprt1* in the WP-AGIQ group compared with that in the untreated controls.

Figure 6 summarizes the directions of the transcript-level changes in the WP-AGIQ group in comparison with

those in the untreated controls in adult stage tests 1 and 2. For most genes, the expression changes were different between adult stage tests 1 and 2, many of them showing an inverse expression pattern, and some genes showed upregulation or downregulation in just one test, except for *Kif21b*, which was upregulated in both tests.

Prelimbic mPFC: In adult stage test 1, compared with the levels in the untreated controls, the transcript level of *Fos* was significantly increased after normalization with *Hprt1* in the PW-AGIQ group, while the transcript level of *Grin2d* was significantly decreased after normalization with *Gapdh* (Fig. 5, Supplementary Table 14: online only). In the DEV-AGIQ group, compared with the levels in the untreated controls, the transcript levels of *Efnb3*, *Ephb1*, *Ephb2*, *Gria1*, *Grin2d*, *Slc17a6*, *Mapk1*, *Notch1*, *Nos1*, and *Nos2* were significantly increased after normalization with

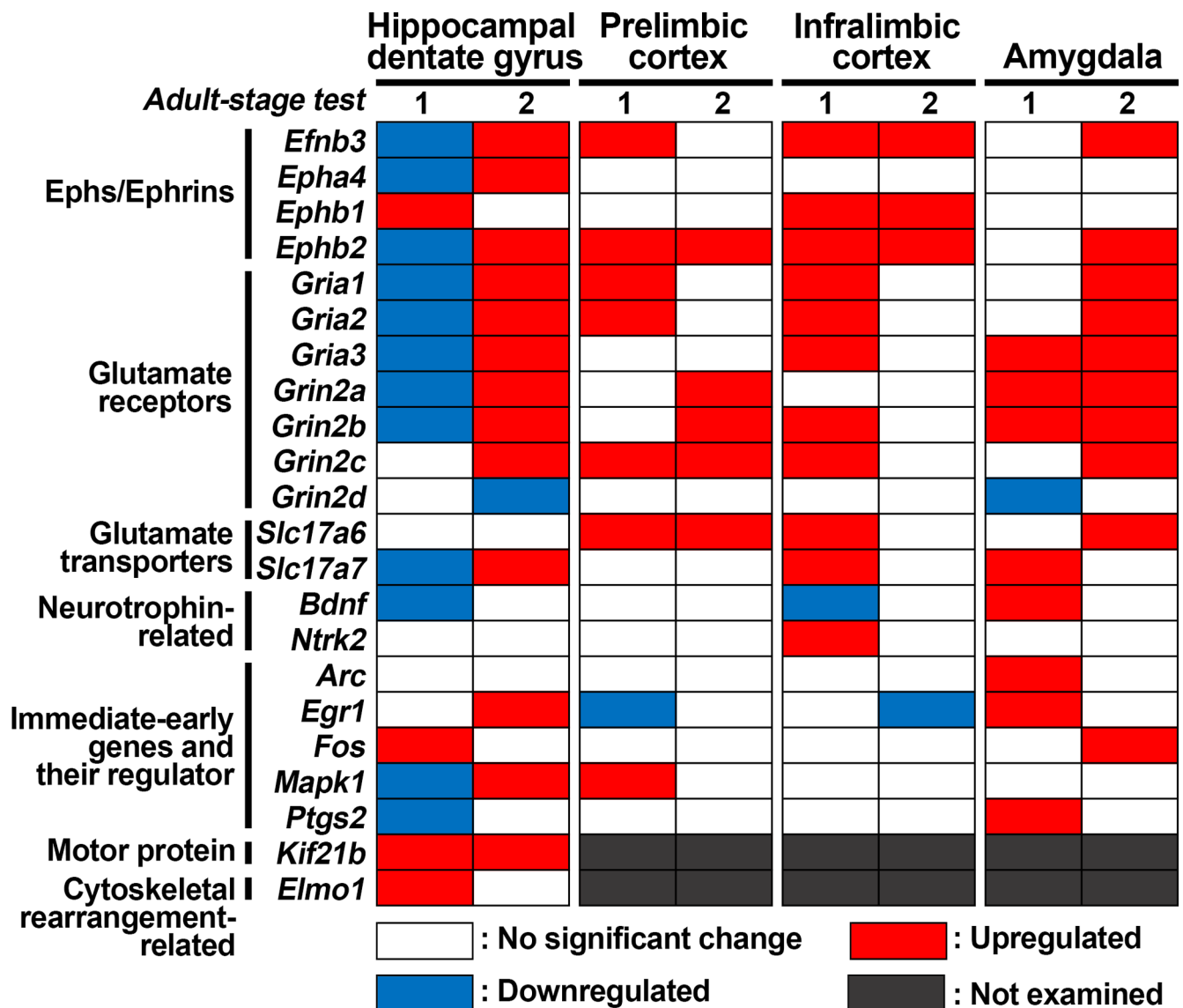


Fig. 6. Comparison of changes in transcript levels between adult stage tests 1 and 2 in specified brain regions of whole period AGIQ-exposed group (WP-AGIQ) rats. Genes with higher or lower transcript levels than those in the untreated controls after normalization with either or both glyceraldehyde-3-phosphate dehydrogenase (*Gapdh*) and hypoxanthine phosphoribosyltransferase 1 (*Hprt1*) were judged to be upregulated or downregulated, respectively.

Gapdh and/or *Hprt1*, while the transcript levels of *Egr1* and *Flt1* were significantly decreased after normalization with *Gapdh*. In the WP-AGIQ group, compared with the levels in the untreated controls, the transcript levels of *Efnb3*, *Ephb2*, *Gria1*, *Gria2*, *Grin2c*, *Slc17a6*, *Mapk1*, *Nos1*, and *Nos3* were significantly increased after normalization with *Gapdh* and *Hprt1*, while the transcript level of *Egr1* was significantly decreased after normalization with *Gapdh*.

In adult stage test 2, the transcript levels of *Ephb2*, *Grin2a*, *Grin2b*, *Grin2c*, and *Slc17a6* in the WP-AGIQ group were significantly increased after normalization with *Hprt1* compared with the levels in the untreated controls (Supplementary Table 15: online only).

Figure 6 summarizes the directions of the transcript-

level changes in the prelimbic cortex in the WP-AGIQ group in comparison with those in the untreated controls between adult stage tests 1 and 2. For many genes, the expression changes were different between adult stage tests 1 and 2, showing upregulation or downregulation in just one test, except for *Ephb2*, *Grin2c*, and *Slc17a6*, which were upregulated in both tests.

Infralimbic mPFC: In adult stage test 1, the transcript level of *Grin2d* in the PW-AGIQ group was significantly decreased after normalization with *Gapdh* compared with that in the untreated controls (Fig. 5, Supplementary Table 16: online only). In the DEV-AGIQ group, compared with the levels in the untreated controls, the transcript levels of *Efnb3*, *Gria1*, *Slc17a6*, and *Pena* were significantly in-

creased after normalization with *Gapdh* and/or *Hprt1*, while the transcript levels of *Epha4* and *Bdnf* were significantly decreased after normalization with *Hprt1*. In the WP-AGIQ group, compared with the levels in the untreated controls, the transcript levels of *Efnb3*, *Ephb1*, *Ephb2*, *Grial1*, *Gria2*, *Gria3*, *Grin2b*, *Grin2c*, *Slc17a6*, *Slc17a7*, *Ntrk2*, *Flt1*, *Kdr*, *Notch1*, *Vegfa*, *Pcna*, *Nos2*, and *Nos3* were significantly increased after normalization with *Gapdh* and/or *Hprt1*, while the transcript level of *Bdnf* was significantly decreased after normalization with *Hprt1*.

In adult stage test 2, the transcript levels of *Efnb3*, *Ephb1*, and *Ephb2* in the WP-AGIQ group were significantly increased after normalization with *Hprt1* compared with those in the untreated controls (Supplementary Table 17: online only). The transcript level of *Egr1* in the WP-AGIQ group was significantly decreased after normalization with *Gapdh* and *Hprt1* compared with that in the untreated controls.

Figure 6 summarizes the directions of the transcript-level changes in the WP-AGIQ group compared with those in the untreated controls between adult stage tests 1 and 2. For many genes, the expression changes were different between adult stage tests 1 and 2, with most of them showing upregulation in just test 1, except for *Efnb3*, *Ephb1*, and *Ephb2*, which were upregulated in both tests.

Amygdala: In adult stage test 1, the transcript level of *Grin2d* in the PW-AGIQ group was significantly decreased after normalization with *Gapdh* and *Hprt1* compared with that in the untreated controls (Fig. 5, Supplementary Table 18: online only). In the DEV-AGIQ group, the transcript levels of *Egr1* and *Ptgs2* were significantly increased after normalization with *Gapdh* compared with those in the untreated controls. In the WP-AGIQ group, compared with the levels in the untreated controls, the transcript levels of *Gria3*, *Grin2a*, *Grin2b*, *Slc17a7*, *Bdnf*, *Arc*, *Egr1*, and *Ptgs2* were significantly increased after normalization with *Gapdh* and/or *Hprt1*, while the transcript levels of *Grin2d* and *Vegfa* were significantly decreased after normalization with *Hprt1*.

In adult stage test 2, the transcript levels of *Efnb3*, *Ephb2*, *Grial1*, *Gria2*, *Gria3*, *Grin2a*, *Grin2b*, *Grin2c*, *Slc17a6*, and *Fos* in the WP-AGIQ group were significantly increased after normalization with *Gapdh* and/or *Hprt1* compared with the levels in the untreated controls (Supplementary Table 19: online only).

Figure 6 summarizes the directions of the transcript-level changes in the WP-AGIQ group compared with those in the untreated controls between adult stage tests 1 and 2. For many genes, the expression changes were different between adult stage tests 1 and 2, showing upregulation or downregulation in just one test, except for *Gria3*, *Grin2a*, and *Grin2b*, which were upregulated in both tests.

Discussion

The adult stage test 1 results of the present study revealed that whole period exposure to AGIQ from the fetal stage to adulthood facilitated fear extinction learning in the

contextual fear conditioning test, which was consistent with the findings in our previous study⁹. Conversely, postweaning or developmental AGIQ exposure did not result in any obvious changes in behavior on our tests. Whole period exposure to AGIQ did not result in any changes to other behavioral parameters, which was also consistent with the findings of our previous study⁹. We also did not observe any behavioral changes in the prepubertal stage test after developmental AGIQ exposure. These results suggest that whole period exposure is necessary for facilitating fear extinction learning, but it may not influence other types of behavior or memory.

The adult stage test 1 results of the present study revealed that postweaning AGIQ exposure did not induce any changes in the transcript levels of most of the genes examined. Conversely, both developmental exposure and whole period exposure to AGIQ resulted in similar changes in transcript levels, notably in the hippocampal dentate gyrus and prelimbic cortex. However, developmental AGIQ exposure did not affect fear extinction learning. These results suggest that AGIQ exposure during development can change the expression levels of genes in adulthood even after exposure has stopped. The ingestion of polyphenols such as quercetin and resveratrol has been reported to be effective in preventing various diseases through epigenetic modifications in the body²⁸. Because large-scale remodeling of the epigenetic landscape occurs in developing cells, developmental AGIQ exposure may modify epigenetic gene regulation. Conversely, whole period exposure to AGIQ altered the expression levels of more genes than did developmental exposure, especially in the infralimbic cortex and the amygdala. Changes in expression caused by developmental exposure might not be sufficient to change behavior as it was measured in the present study. Genes with altered expression only after whole period exposure might be related to the facilitation of fear extinction learning.

After adult stage tests 1 and 2, we found an increased number of FOS⁺ neurons in the infralimbic cortex of rats that experienced whole period exposure to AGIQ. While the reason for the lack of spontaneous recovery of fear responses in the untreated controls is not clear, whole period exposure did not modify the lack of spontaneous recovery observed in adult stage test 1, which suggests that the behavioral test used in this study might not activate the corresponding neural circuit. This result further suggests that changes in transcript levels after the spontaneous recovery test may be equivalent to the changes in constitutive expression that occur without the behavioral stimulus. From this point of view, the increased number of FOS⁺ neurons in the infralimbic cortex may represent constitutive upregulation that was not influenced by the behavioral test and instead reflects strengthening of basal level synaptic plasticity in the infralimbic cortex caused by AGIQ. Unlike FOS⁺ neurons, we found an increased number of p-ERK1/2⁺ neurons in both the prelimbic and infralimbic cortices after adult stage test 2. A subset of plasticity-evoked and stimuli-induced IEGs have been implicated in the formation of memory

traces that occur after learning because of their rapid and transient responsiveness to synaptic activation¹⁴. Therefore, synaptic plasticity-related IEGs and their regulator, p-ERK1/2, which showed altered expression or activity after the learning trial, could be involved in the facilitation of fear extinction learning. In particular, molecules that showed increased expression or activity only after adult stage test 2 and not after adult stage test 1 might be essential for the facilitation of fear extinction learning by AGIQ. ERK1/2 can be rapidly activated by phosphorylation in response to acute stimuli to induce IEGs to participate in the facilitation of synaptic plasticity²⁹. Therefore, the activation of ERK1/2 only after adult stage test 2 may be essential for facilitating fear extinction learning by enhancing synaptic plasticity. The prelimbic and infralimbic cortices have been proposed to accelerate and suppress fear responses, respectively¹³. However, a recent study has shown that activation of the prelimbic cortex neurons, which project to the infralimbic cortex, promotes fear extinction learning³⁰. Therefore, our results from the immunohistochemical analysis of induced proteins suggest that the high response seen in the learning-dependent activation of ERK1/2 in the prelimbic and infralimbic cortices contributes to the facilitation of fear extinction learning as a result of AGIQ exposure from the fetal stage to adulthood. Alternatively, the fear memory formation could be translated into a psychological toxic insult, and AGIQ exposure could establish new learning-related neural circuits in both the prelimbic and infralimbic cortices that function to facilitate the extinction of fear memory as a result of psychological toxicity.

In the infralimbic cortex after adult stage test 1, whole period exposure to AGIQ preferentially upregulated a number of genes, such as *Gria2*, *Gria3*, *Grin2b*, *Grin2c*, *Slc17a7*, *Ntrk2*, *Ftl1*, *Kdr*, *Notch1*, *Vegfa*, *Nos2*, and *Nos3*, relative to developmental exposure. *Gria* is a gene family comprising glutamate ionotropic receptor alpha-amino-3-hydroxy-5-methyl-4-isoxazolepropionic acid (AMPA)-type subunits 1 to 4. These receptors are found at excitatory synapses throughout the brain³¹. *Slc17a7* encodes vesicular glutamate transporter (VGLUT)-1, one of the major isoforms of VGLUTs³². BDNF/TrkB has also been shown to regulate VGLUT expression during development, and its effect on VGLUT1 may contribute to enhancing glutamate release in long-term potentiation³³. The BDNF/TrkB receptor complex upregulates *Grial*, *Gria2*, and *Gria3*³⁴, and these modifications enhance synaptic strength³⁵. *Grin2* encodes glutamate ionotropic receptor NMDA-type subunit of GluN2, and the NMDA receptor is a tetramer that consists of two GluN1 subunits combined with two GluN2 subunits or a mixture of a GluN2 and a GluN3 subunit³⁶. NMDA receptors are critical for inducing long-term potentiation³⁶. Furthermore, D-cycloserine-induced facilitation of fear extinction learning was found to increase FOS⁺ neurons and upregulate NMDA receptors in both the prelimbic and infralimbic cortices³⁷. Although we found increased numbers of FOS⁺ neurons only in the infralimbic cortex, the observed changes in gene expression also support the strengthening of the basal

level of synaptic plasticity of glutamatergic signals in the infralimbic cortex.

Ftl1, *Kdr*, *Notch1*, *Vegfa*, and *Nos3*, have been shown to be involved in increasing blood flow through the brain via enhanced angiogenesis or dilatation of blood vessels^{38–40}. Flavonoids are known to activate nitric oxide synthase 3, which is encoded by *Nos3*⁴¹. *Nos2* encodes nitric oxide synthase 2 (NOS2), which is expressed in neurons and glia of the brain⁴². Nitric oxide acts as an intracellular neurotransmitter that modulates synaptic plasticity in several types of neurons⁴². Inhibition of NOS2 has also been reported to reduce spontaneous and evoked synaptic activity in the neocortex⁴³. Therefore, the observed changes in expression also suggest the strengthening of the basal level of synaptic plasticity and blood flow in the infralimbic cortex.

In the amygdala, whole period exposure to AGIQ preferentially upregulated a number of genes after adult stage test 1 relative to developmental exposure, including *Gria3*, *Grin2a*, *Grin2b*, *Slc17a7*, *Bdnf*, and *Arc*. As mentioned, the BDNF/TrkB receptor complex upregulates *Gria3* as well as *Slc17a7*^{33, 34}. ARC has been reported to interact with endocytic machinery to regulate AMPA receptor trafficking and contribute to synaptic plasticity⁴⁴. Therefore, the observed changes in expression found here also suggest the strengthening of the basal level of synaptic plasticity in the amygdala.

Whole period exposure to AGIQ upregulated a number of genes, especially in the hippocampal dentate gyrus and amygdala, after adult stage test 2 that were unchanged or downregulated after adult stage test 1. In the hippocampal dentate gyrus, upregulation was observed for *Efnb3*, *Epha4*, *Ephb2*, *Grial*, *Gria2*, *Gria3*, *Grin2a*, *Grin2b*, *Grin2c*, *Slc17a7*, *Egr1*, and *Mapk1*. *Efnb* and *Eph* encode an Ephrin ligand and Eph receptor family, and Ephrin and Eph are classified into two subgroups: EphrinA or EphrinB and EphA or EphB, respectively⁴⁵. EphA4 and EphB2 regulate NMDA and AMPA receptor functions and neuronal morphology, which are believed to function in memory formation⁴⁵. Previously, we observed reduced number of EphA4⁺ cells in the GCL at the end of developmental hypothyroidism induced by maternally administered 6-propyl-2-thiouracil (PTU), and in turn, an increased number of EphA4⁺ cells in the GCL was observed at the adult stage after cessation of PTU exposure, in parallel with the increased number of ARC⁺ cells in the GCL⁴⁶. These results may suggest enhanced synaptic plasticity mediated by ARC and involving Eph induction at the adult stage. As mentioned above, AMPA receptors, NMDA receptors, and VGLUT1 are involved in synaptic plasticity. Moreover, *Egr1* encodes an IEG and is known to be involved in modulating synaptic plasticity^{10, 47}. Furthermore, *Mapk1* encodes a member of the MAPK protein family, ERK2, that is crucial for regulating synaptic plasticity⁴⁸. In the amygdala, the upregulation of *Slc17a6* and *Fos* was observed, in addition to the upregulation of *Efnb3*, *Ephb2*, *Grial*, *Gria2*, and *Grin2c* in the hippocampal dentate gyrus. *Slc17a6* encodes VGLUT2, which is one of the major VGLUT isoforms and acts as a glutamate transporter in glu-

tamatergic neurons³². Therefore, genes upregulated in the hippocampal dentate gyrus and amygdala specifically after adult stage test 2 may be involved in the enhancement of learning-dependent synaptic plasticity by AGIQ exposure.

We previously found transcript upregulation of *Fos* in the hippocampal dentate gyrus and of *Grin2d* in the amygdala after whole period exposure to AGIQ⁹. AGIQ also increased the number of FOS⁺ hippocampal granule cells. In that study, we examined immunohistochemical cellular number in animals that were not subjected to behavioral tests. In the present study, while the change was not statistically significant, we observed more FOS⁺ granule cells after whole period exposure than that in the untreated controls after adult stage test 1. Moreover, increased *Fos* transcript levels were observed in the hippocampal dentate gyrus in these animals. These results are similar to those of our previous study⁹. Conversely, the *Grin2d* transcript level in the amygdala after whole period exposure in the present study was unchanged or lower than what was observed in the untreated controls in adult stage tests 1 and 2. This was inconsistent with the results of our previous study. Although the reason why the increased expression of *Grin2d* in the amygdala was not reproduced is unclear, genes encoding other NMDA receptor-subunits were upregulated after both adult stage tests in the present study.

We previously found increased transcript levels of *Kif21b* in the hippocampal dentate gyrus after whole period exposure to AGIQ⁹. In the present study, similar findings were obtained after both adult stage tests 1 and 2, which suggests the constitutive upregulation of *Kif21b*. Furthermore, we found increased transcript levels of *Elmol* after adult stage test 1 in rats that experienced whole period exposure. *Elmol* encodes engulfment and cell motility 1 (ELMO1), which along with KIF21B has been reported to control long-term depression through modulation of the RAC1 activation/inactivation cycle in the hippocampus¹². Therefore, these results suggest that an enhanced RAC1 activation/inactivation cycle through the upregulation of ELMO1 and KIF21B may also contribute to the facilitation of fear extinction learning.

In conclusion, the present study revealed that continuous exposure to AGIQ from the fetal stage to adulthood is necessary for facilitating fear extinction learning at the adult stage. Immunohistochemical and gene-expression analyses revealed that facilitation of extinction might involve both constitutive and learning-dependent upregulation of synaptic plasticity-related genes/proteins which are likely differentially involved in the brain regions regulating fear memory. In particular, the results suggest that new learning-related neural circuits for facilitating fear extinction could be established in the mPFC.

Disclosure of Potential Conflicts of Interest: Mihoko Koyanagi and Shim-mo Hayashi are employed by a food additive manufacturer whose product lines include α -glycosyl isoquercitrin. Robert R. Maronpot is a scientific consultant at the aforementioned food additive manufacturer. The

views and opinions expressed in this article are those of the authors and not necessarily those of their respective employers. Yasunori Masubuchi, Junta Nakahara, Satomi Kikuchi, Hiromu Okano, Yasunori Takahashi, Kazumi Takashima, Toshinori Yoshida, and Makoto Shibutani declare that no competing interests exist.

Acknowledgments: The authors thank Mrs. Shigeko Suzuki for her technical assistance in preparing the histological specimens. This work was supported by San-Ei Gen F.F.I., Inc.

References

1. Akiyama T, Washino T, Yamada T, Koda T, and Maitani T. Constituents of enzymatically modified isoquercitrin and enzymatically modified rutin (extract). *J. Food Hyg Safe Sci.* **41**: 54–60. 2000. [[CrossRef](#)]
2. Formica JV, and Regelson W. Review of the biology of Quercetin and related bioflavonoids. *Food Chem Toxicol.* **33**: 1061–1080. 1995. [[Medline](#)] [[CrossRef](#)]
3. Kangawa Y, Yoshida T, Abe H, Seto Y, Miyashita T, Nakamura M, Kihara T, Hayashi SM, and Shibutani M. Anti-inflammatory effects of the selective phosphodiesterase 3 inhibitor, cilostazol, and antioxidants, enzymatically-modified isoquercitrin and α -lipoic acid, reduce dextran sulphate sodium-induced colorectal mucosal injury in mice. *Exp Toxicol Pathol.* **69**: 179–186. 2017. [[Medline](#)] [[CrossRef](#)]
4. Gasparotto Junior A, Gasparotto FM, Lourenço EL, Crestani S, Stefanello ME, Salvador MJ, da Silva-Santos JE, Marques MC, and Kassuya CA. Antihypertensive effects of isoquercitrin and extracts from *Tropaeolum majus* L.: evidence for the inhibition of angiotensin converting enzyme. *J Ethnopharmacol.* **134**: 363–372. 2011. [[Medline](#)] [[CrossRef](#)]
5. Makino T, Kanemaru M, Okuyama S, Shimizu R, Tanaka H, and Mizukami H. Anti-allergic effects of enzymatically modified isoquercitrin (α -oligoglucosyl quercetin 3-*O*-glucoside), quercetin 3-*O*-glucoside, α -oligoglucosyl rutin, and quercetin, when administered orally to mice. *J Nat Med.* **67**: 881–886. 2013. [[Medline](#)] [[CrossRef](#)]
6. Fujii Y, Kimura M, Ishii Y, Yamamoto R, Morita R, Hayashi SM, Suzuki K, and Shibutani M. Effect of enzymatically modified isoquercitrin on preneoplastic liver cell lesions induced by thioacetamide promotion in a two-stage hepatocarcinogenesis model using rats. *Toxicology.* **305**: 30–40. 2013. [[Medline](#)] [[CrossRef](#)]
7. Nyska A, Hayashi SM, Koyanagi M, Davis JP, Jokinen MP, Ramot Y, and Maronpot RR. Ninety-day toxicity and single-dose toxicokinetics study of α -glycosyl isoquercitrin in Sprague-Dawley rats. *Food Chem Toxicol.* **97**: 354–366. 2016. [[Medline](#)] [[CrossRef](#)]
8. Hobbs CA, Koyanagi M, Swartz C, Davis J, Kasamoto S, Maronpot R, Recio L, and Hayashi SM. Comprehensive evaluation of the flavonol anti-oxidants, α -glycosyl isoquercitrin and isoquercitrin, for genotoxic potential. *Food Chem Toxicol.* **113**: 218–227. 2018. [[Medline](#)] [[CrossRef](#)]
9. Okada R, Masubuchi Y, Tanaka T, Nakajima K, Masuda S, Namamura K, Maronpot RR, Yoshida T, Koyanagi M, Hayashi SM, and Shibutani M. Continuous exposure to

- α -glycosyl isoquercitrin from developmental stage facilitates fear extinction learning in rats. *J Funct Foods*. **55**: 312–324. 2019. [[CrossRef](#)]
10. Guzowski JF. Insights into immediate-early gene function in hippocampal memory consolidation using antisense oligonucleotide and fluorescent imaging approaches. *Hippocampus*. **12**: 86–104. 2002. [[Medline](#)] [[CrossRef](#)]
 11. Harney SC, Jane DE, and Anwyl R. Extrasynaptic NR2D-containing NMDARs are recruited to the synapse during LTP of NMDAR-EPSCs. *J Neurosci*. **28**: 11685–11694. 2008. [[Medline](#)] [[CrossRef](#)]
 12. Morikawa M, Tanaka Y, Cho HS, Yoshihara M, and Hirokawa N. The molecular motor KIF21B mediates synaptic plasticity and fear extinction by terminating racl activation. *Cell Rep*. **23**: 3864–3877. 2018. [[Medline](#)] [[CrossRef](#)]
 13. Maren S, Phan KL, and Liberzon I. The contextual brain: implications for fear conditioning, extinction and psychopathology. *Nat Rev Neurosci*. **14**: 417–428. 2013. [[Medline](#)] [[CrossRef](#)]
 14. Minatohara K, Akiyoshi M, and Okuno H. Role of immediate-early genes in synaptic plasticity and neuronal ensembles underlying the memory trace. *Front Mol Neurosci*. **8**: 78. 2016. [[Medline](#)] [[CrossRef](#)]
 15. Lee B, Shim I, Lee H, and Hahm DH. Effects of epigallocatechin gallate on behavioral and cognitive impairments, hypothalamic-pituitary-adrenal axis dysfunction, and alternations in hippocampal BDNF expression under single prolonged stress. *J Med Food*. **21**: 979–989. 2018. [[Medline](#)] [[CrossRef](#)]
 16. Zhang ZS, Qiu ZK, He JL, Liu X, Chen JS, and Wang YL. Resveratrol ameliorated the behavioral deficits in a mouse model of post-traumatic stress disorder. *Pharmacol Biochem Behav*. **161**: 68–76. 2017. [[Medline](#)] [[CrossRef](#)]
 17. Monsey MS, Gerhard DM, Boyle LM, Briones MA, Seligsohn M, and Schafe GE. A diet enriched with curcumin impairs newly acquired and reactivated fear memories. *Neuropsychopharmacology*. **40**: 1278–1288. 2015. [[Medline](#)] [[CrossRef](#)]
 18. Tapias-Espinosa C, Kádár E, and Segura-Torres P. Spaced sessions of avoidance extinction reduce spontaneous recovery and promote infralimbic cortex activation. *Behav Brain Res*. **336**: 59–66. 2018. [[Medline](#)] [[CrossRef](#)]
 19. Milad MR, Igoe SA, Lebron-Milad K, and Novales JE. Estrous cycle phase and gonadal hormones influence conditioned fear extinction. *Neuroscience*. **164**: 887–895. 2009. [[Medline](#)] [[CrossRef](#)]
 20. Mora S, Dussaubat N, and Díaz-Véliz G. Effects of the estrous cycle and ovarian hormones on behavioral indices of anxiety in female rats. *Psychoneuroendocrinology*. **21**: 609–620. 1996. [[Medline](#)] [[CrossRef](#)]
 21. Paris JJ, and Frye CA. Estrous cycle, pregnancy, and parity enhance performance of rats in object recognition or object placement tasks. *Reproduction*. **136**: 105–115. 2008. [[Medline](#)] [[CrossRef](#)]
 22. Kovács KJ. Measurement of immediate-early gene activation- c-fos and beyond. *J Neuroendocrinol*. **20**: 665–672. 2008. [[Medline](#)] [[CrossRef](#)]
 23. Chen C, Magee JC, and Bazan NG. Cyclooxygenase-2 regulates prostaglandin E₂ signaling in hippocampal long-term synaptic plasticity. *J Neurophysiol*. **87**: 2851–2857. 2002. [[Medline](#)] [[CrossRef](#)]
 24. Brami-Cherrier K, Roze E, Girault JA, Betuing S, and Caboche J. Role of the ERK/MSK1 signalling pathway in chromatin remodelling and brain responses to drugs of abuse. *J Neurochem*. **108**: 1323–1335. 2009. [[Medline](#)] [[CrossRef](#)]
 25. Paxinos G, and Watson C. *The Rat Brain in Stereotaxic Coordinates* 7th ed. Academic Press, Massachusetts. figures 11 and 58. 2014.
 26. Akane H, Saito F, Yamanaka H, Shiraki A, Imatanaka N, Akahori Y, Morita R, Mitsumori K, and Shibutani M. Methacarn as a whole brain fixative for gene and protein expression analyses of specific brain regions in rats. *J Toxicol Sci*. **38**: 431–443. 2013. [[Medline](#)] [[CrossRef](#)]
 27. Livak KJ, and Schmittgen TD. Analysis of relative gene expression data using real-time quantitative PCR and the 2-^{- $\Delta\Delta C_T$} Method. *Methods*. **25**: 402–408. 2001. [[Medline](#)] [[CrossRef](#)]
 28. Ayissi VBO, Ebrahimi A, and Schluesener H. Epigenetic effects of natural polyphenols: a focus on SIRT1-mediated mechanisms. *Mol Nutr Food Res*. **58**: 22–32. 2014. [[Medline](#)] [[CrossRef](#)]
 29. Gao YJ, and Ji RR. c-Fos and pERK, which is a better marker for neuronal activation and central sensitization after noxious stimulation and tissue injury? *Open Pain J*. **2**: 11–17. 2009. [[Medline](#)] [[CrossRef](#)]
 30. Marek R, Xu L, Sullivan RKP, and Sah P. Excitatory connections between the prelimbic and infralimbic medial prefrontal cortex show a role for the prelimbic cortex in fear extinction. *Nat Neurosci*. **21**: 654–658. 2018. [[Medline](#)] [[CrossRef](#)]
 31. Ozawa S, Kamiya H, and Tsuzuki K. Glutamate receptors in the mammalian central nervous system. *Prog Neurobiol*. **54**: 581–618. 1998. [[Medline](#)] [[CrossRef](#)]
 32. Liguz-Lecznar M, and Skangiel-Kramska J. Vesicular glutamate transporters (VGLUTs): the three musketeers of glutamatergic system. *Acta Neurobiol Exp (Wars)*. **67**: 207–218. 2007. [[Medline](#)]
 33. Melo CV, Mele M, Curcio M, Comprido D, Silva CG, and Duarte CB. BDNF regulates the expression and distribution of vesicular glutamate transporters in cultured hippocampal neurons. *PLoS One*. **8**: e53793. 2013. [[Medline](#)] [[CrossRef](#)]
 34. Caldeira MV, Melo CV, Pereira DB, Carvalho R, Correia SS, Backos DS, Carvalho AL, Esteban JA, and Duarte CB. Brain-derived neurotrophic factor regulates the expression and synaptic delivery of alpha-amino-3-hydroxy-5-methyl-4-isoxazole propionic acid receptor subunits in hippocampal neurons. *J Biol Chem*. **282**: 12619–12628. 2007. [[Medline](#)] [[CrossRef](#)]
 35. Korte M, Kang H, Bonhoeffer T, and Schuman E. A role for BDNF in the late-phase of hippocampal long-term potentiation. *Neuropharmacology*. **37**: 553–559. 1998. [[Medline](#)] [[CrossRef](#)]
 36. Yamamoto H, Hagino Y, Kasai S, and Ikeda K. Specific roles of NMDA receptor subunits in mental disorders. *Curr Mol Med*. **15**: 193–205. 2015. [[Medline](#)] [[CrossRef](#)]
 37. Gupta SC, Hillman BG, Prakash A, Ugale RR, Stairs DJ, and Dravid SM. Effect of D-cycloserine in conjunction with fear extinction training on extracellular signal-regulated kinase activation in the medial prefrontal cortex and amygdala in rat. *Eur J Neurosci*. **37**: 1811–1822. 2013. [[Medline](#)] [[CrossRef](#)]
 38. Plate KH. Mechanisms of angiogenesis in the brain. *J Neuropathol Exp Neurol*. **58**: 313–320. 1999. [[Medline](#)] [[CrossRef](#)]

Ref]

39. Takeshita K, Satoh M, Ii M, Silver M, Limbourg FP, Mukai Y, Rikitake Y, Radtke F, Gridley T, Losordo DW, and Liao JK. Critical role of endothelial Notch1 signaling in post-natal angiogenesis. *Circ Res.* **100**: 70–78. 2007. [[Medline](#)] [[CrossRef](#)]
40. Tousoulis D, Kampoli AM, Tentolouris C, Papageorgiou N, and Stefanadis C. The role of nitric oxide on endothelial function. *Curr Vasc Pharmacol.* **10**: 4–18. 2012. [[Medline](#)] [[CrossRef](#)]
41. Spencer JPE, Vauzour D, and Rendeiro C. Flavonoids and cognition: the molecular mechanisms underlying their behavioural effects. *Arch Biochem Biophys.* **492**: 1–9. 2009. [[Medline](#)] [[CrossRef](#)]
42. Hardingham N, Dachtler J, and Fox K. The role of nitric oxide in pre-synaptic plasticity and homeostasis. *Front Cell Neurosci.* **7**: 190. 2013. [[Medline](#)] [[CrossRef](#)]
43. Buskila Y, and Amitai Y. Astrocytic iNOS-dependent enhancement of synaptic release in mouse neocortex. *J Neurophysiol.* **103**: 1322–1328. 2010. [[Medline](#)] [[CrossRef](#)]
44. Chowdhury S, Shepherd JD, Okuno H, Lyford G, Petralia RS, Plath N, Kuhl D, Huganir RL, and Worley PF. Arc/Arg3.1 interacts with the endocytic machinery to regulate AMPA receptor trafficking. *Neuron.* **52**: 445–459. 2006. [[Medline](#)] [[CrossRef](#)]
45. Dines M, and Lamprecht R. The role of ephs and ephrins in memory formation. *Int J Neuropsychopharmacol.* **19**: pyv106. 2016. [[Medline](#)] [[CrossRef](#)]
46. Shiraki A, Tanaka T, Watanabe Y, Saito F, Akahori Y, Imatanaka N, Yoshida T, and Shibutani M. Immunohistochemistry of aberrant neuronal development induced by 6-propyl-2-thiouracil in rats. *Toxicol Lett.* **261**: 59–71. 2016. [[Medline](#)] [[CrossRef](#)]
47. Duclot F, and Kabbaj M. The role of early growth response 1 (EGR1) in brain plasticity and neuropsychiatric disorders. *Front Behav Neurosci.* **11**: 35. 2017. [[Medline](#)] [[CrossRef](#)]
48. Thomas GM, and Huganir RL. MAPK cascade signalling and synaptic plasticity. *Nat Rev Neurosci.* **5**: 173–183. 2004. [[Medline](#)] [[CrossRef](#)]